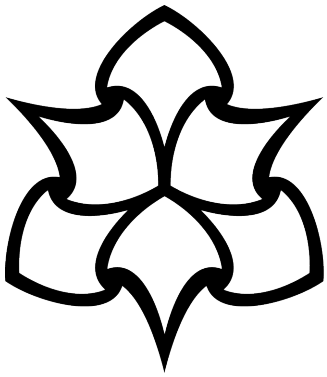

An Efficient Monitoring of Eclamptic Seizures in Wireless Sensors Networks

Daniyal Haider[a], Aifeng Ren[b], Dou Fan[b], Nan Zhao[b], Xiaodong Yang[b]*,

Syed Aziz Shah[a,c], Fangming Hu[b], Qammer H. Abbasi[c]

[a]*School of International Education, Xidian University, 2 South Taibai Road, Xi'an, Shaanxi, 710071, China*
[b]*School of Electronic Engineering, Xidian University, 2 South Taibai Road, Xi'an, Shaanxi, 710071, China*
[c]*School of Engineering, University of Glasgow, Glasgow G12 8QQ, UK*
Corresponding author: Xiaodong Yang; Email: xdyang@xidian.edu.cn

Abstract: This paper presents the application of wireless sensing at C-band operating at 4.8 GHz technology (a potential Chinese 5G band). A wireless transceiver is used in the indoor environment to monitor different body motions of a woman experiencing an eclamptic seizure. The body movement shows unique wireless data which carries the wireless channel information. The results indicate that using higher features increases the accuracy from 3% to 4% for classifying data from different body motions. All of the four classifiers are compared by using six performance metrics such as accuracy, recall, precession, specificity, F-measure and Kappa. The values from these metrics indicate the better performance of SVM as compared to other three classifiers, the results indicate that the eclamptic seizures are easily differentiated from other body movements by applying the aforementioned classifiers.

Index Terms- C-band, Wireless channel information (WCI), Internet of Thing (IoT), support vector machine (SVM), K-Nearest Neighbor (KNN), Random Forest (RF) and K-Mean.

1. Introduction

The journey towards reliable communication leads us to 5G, which has totally changed the standards for wireless communication and as a result demand for the stable and high quality communication has increased. In wireless communication, 5G is the next communication standard that has many advantages such as supporting applications like enhance mobile broadband (eMBB), ultra-reliable low latency communication (URLLC) and indoor wireless sensing. [1]. The 5G sensing system has maximum potential with greater monitoring capabilities in public and private areas. In general, monitoring [2] the people in a crowded area, security of a house and investigating the crime scene etc. The 5G sensing networks operating at 4.8 GHz has greater potential for multi-modal communication with the high ratio of quality of experience (QoE) [3-4].

Presently, non-invasive wireless sensing plays a key role in the health sector. This improves the medical industry and raises the standards of the health sector by providing good medical attention to the patients and reducing the cost for providing the best medical facilities. The wireless sensing technology has greater importance in medical industry by providing remote medical care at homes or on move [2]. It also reduces the cost of providing different medical services by using 5G technology. The 5G sensing leveraging C-band is the new era in medical industry for monitoring patients and reduces the cost for health care with reliable monitoring of patients and diagnoses [3-4].

The proposed method deals with the monitoring of patients suffering from a disease known as Eclampsia, experienced by pregnant woman. Hypertension is one of the conditions experienced by the eclampsia disease patient. During the pregnancy period, hypertension is the most and common complication related to the woman pregnancy. This has larger contribution in the maternal morbidity and also in the fetal mortality. This is also known as Pregnancy Induced Hypertension, (PIH). PIH, inducing complication rate is very high as compared to other pregnancy related problem, as it complicates one out of every tenth pregnancy [5].

According to many studies and authorities such as American college of Obstetrician and Gynecology, hypertension has many induced forms like gestational hypertension, pre-eclampsia and eclampsia. Pre-eclampsia is one of the important and sever form of PIH [9]. It is the multi-system disorder of PIH with unknown cause and appears after the 20^{th} week of gestation. This can lead to the death of a mother and also to a pre-mature delivery. There are many risks of having pre-eclampsia, it happens more often when a woman has pregnancy with multiple gestations, age more than 35 years, diabetes, obesity or with family history of pre-eclampsia. A lot of symptoms involve in presence of pre-eclampsia, some of them are headache, high blood pressure, abdominal pain, high proteinuria, Tonic-colonic seizures, visual disturbance etc. There are around 50,000 to 60,000 pre-eclampsia deaths per year recorded worldwide [7]. PE has larger effect on the worldwide almost 8% to 15% pregnancies are affected [7]. In United States pre-eclampsia has increased by 25% in past few decades [7].

During the pregnancy, a woman with pre-eclampsia should have controlled blood pressure to avoid organ damage. With uncontrolled condition, there is a high chance of mortality of a mother and fetus. Pre-eclampsia could be characterized into two types, mild and severe [8]. The severe type of pre-eclampsia should be controlled, or it might turn into eclampsia which is the worst form of hypertension. During the state of pregnancy occurrence of seizures, visual disturbance and high blood pressure leads from pre-eclampsia to eclampsia.

Eclampsia needs to be diagnosed as early as possible, hypertensive issues during pregnancy require medical attention and evaluation, as symptoms such as excessive headaches, blurry vision, seizures, vomiting, time to time face, hands and feet swelling directly relates to high blood pressure. The exact cause of pre-eclampsia and eclampsia is still unknown, but there exists number of risks that could develop pregnancy induced hypertension, pre-eclampsia and eclampsia. Studies indicate that the pre-eclampsia and eclampsia occurs during woman first pregnancy. To avoid risk of injury, patient should be under medical observations in a quiet environment. All physiological monitoring and investigations results must be recorded for future monitoring process.

To keep a pregnant woman under observations, a system is presented that continuously monitors the patients and efficiently detects the seizure episodes. The system exploits the small wireless devices such as 4.8 GHz transmitter, omni-directional antenna, and network interface card used in internet of things (IoTs) for 5G technology, and extract the perturbations of wireless channel information. Each human body motion induces a unique imprint that is used to detect the seizure episodes. These body motions are categorized into four classes and for the data classification, we have used different machine learning algorithms including support vector machine (SVM), K-nearest neighbor (KNN), random forest (RF) and K-mean. . Literature review indicates that there exist several systems that detect various body motions but they present several limitations which are explained in section 3.

Table 1: Acronym used in the paper.

Symbols	Abbreviations	Symbols	Abbreviations
WCI	Wireless Channel Information	PIH	Pregnancy Induced Hypertension
SVM	Support Vector Machine	eMBB	Enhance Mobile Broadband
KNN	K-Nearest Neighbour	URLLC	Ultra-Reliable Low Latency Communication
RF	Random Forest	NIC	Network Interface Card

LOS	Line-Of-sight	CFR	Channel Frequency Response
NLOS	Non-Line-Of-sight	AP	Access Point
IoT	internet Of Thing	Tp	True Positive
DM	Data Mining	Tn	True Negative
ML	Machine Learning	Fp	False Positive
RBF	Radial Basis Function	Fn	False Negative

The organization of the paper is as follow, Section 2 the prospective system design. Section 3 presents the prior art. Section 4 cites the multipath challenges. Section 5 cites the implementation of classification algorithms. Section 6 presents the SVM classification scenarios. Section 7 cites the discussion about the results. Section 8 explains the feature extraction and selection and Section 9 shows the performance analysis of algorithms and finally section 10 explains the final conclusion. Moreover, Table 1 show the acronyms used in this paper.

2. Prospective system design

The proposed method uses 5G sensing that operate at 4.8 GHz and exploit the perturbations of wireless channel when the subject makes certain movements. These movements produces a unique wireless channel signature in the form of wireless channel information (WCI) which is extracted using 4.8 GHz transmitter, network interface card and an omni-directional antenna. In wireless transmission, the obstructions result in multiple copies of a signal at receiver side due to multipath propagation.

The human body acts as an obstacle as shown in Figure 1 (experimental setup), as result disturbs the wireless medium and causes the signal to propagation via multiple paths. The received WCI data contain subcarrier frequencies up to 30 subcarriers and characterizes the wireless channel information.

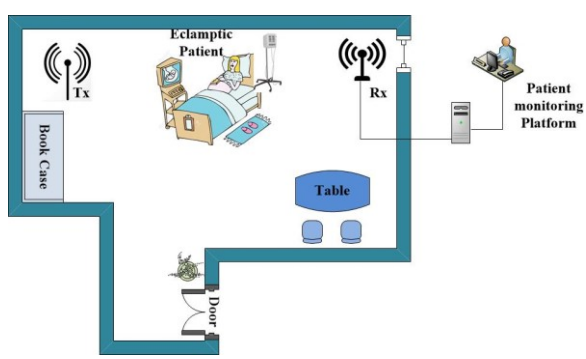

Figure 1: Experimental Overview.

The patient body acts as an obstacle as the signal propagates from transmitter to receiver. The received signal can be written as: $b=Ha + k$, where b represents the signal at receiver side, a as transmitted signal and k as white Gaussian noise. The wireless channel information is stored as a complex number matrix H. The matrix H contains a group of 30 subcarriers (frequency channels), where each subcarrier carries the amplitude and phase information. The wireless signal travels from transmitter to the receiver, follows a straight path which is known as Line-Of-sight (LOS) signal propagation. On the other hand, the Non-Line-Of-Sight (NLOS) signal propagation takes place if there exist any obstacle in the path of radio signal, resulting in many unwanted affects like scattering, multipath fading, reflection and refraction. In each case, the value for Channel Frequency Response (CFR) will be different. The

wireless data received for particular time period is stored as WCI packets. The received packets represent the wireless channel information..

Figure 2 explains the signal propagation through LOS (A) and NLOS (B) and the body posture induces the shift in the signal propagation. In this way, we can record the CFR and can monitor the body motion of the patient after getting the wireless channel information. The data received using 5G sensing is then classified using different classifiers to obtain the percent accuracy and to evaluate the system performance.

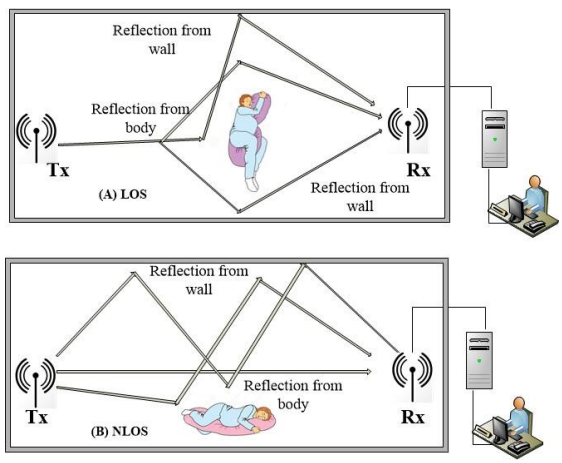

Figure 2: WCI for LOS and NLOS.

The prospective system flow graph is shown in the Figure 3.

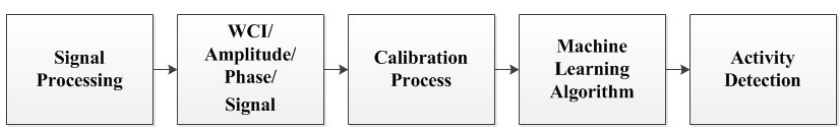

Figure 3: Basic Flow of the System design.

3. Prior Art

Many approaches are used for measuring hypertension, blood pressure during pregnancy and pre-eclampsia. But no direct method is available to detect the eclamptic seizures on time to prevent any harm to the patient. Dustin T. Dunsmuir *et al.* [9] presented an application-based analysis and diagnosis for woman with pre-eclampsia. The idea was to provide an efficient way for community health services to monitor the symptoms and take some clinical measurements for minimizing the risk of eclampsia. The data could be easily monitored on every visit and at any place by using different electronics devices. Oxygen saturation measurement becomes easy by using phone oximeter with the help of this application. Mário W. L. Moreira et al. [10] used Data Mining (DM) technique for extraction of patterns and assisting in the knowledge discovery. Identification of all hypertensive crises becomes easy to avoid the death related issues for the woman. In [10] the comparison of two Bayesian classifiers was presented to predict the hypertensive complexity. G. Williams et al. [11] proposed a telemedicine system to detect the pre-eclampsia that used electronic sensor sleeve, radio telemetry and ring less interface unit directly connected to the PSTN. Data could be measured by hospital computers for monitoring the disease. The sleeve was made of two arrays of infrared LED's along with a detector that measure the blood pressure 20 cm apart. *Kumari L. Fernando et al.* [12] presented another approach of predicting hypertension with the help of coherence analysis. The

research used magnitude squared coherence to analyze the two waveforms and how well they correspond in frequency domain. The analysis shows that values are high in complicated hypertension as compared to non-hypertensive woman. The comparison of different approaches is shown in Table 2.

Table 2: comparison of different approaches for activity detection.

S/N	Techniques for activity detection	Explanation	Advantages	Limitations
1	Camera	Yantao Lu et al. [13] presented the idea of human activity detection with warble devices along with camera. In this the activity is detected by using accelerometer and ego-vision data from smart phone.	Easy to handle, More robust.	Costly, You have to wear the devices, Uncomfortable.
2	Thermal & Infrared	Ting Feng Tan et al. [14] presented the idea of human activity recognition using the thermal and infrared technology. The system uses 4 x 4 thermal sensors and infrared camera. The images from the camera then pass through human detection algorithms to detect the activity.	Effective for larger area, detection time is effective.	Can detect other heat signals, more hardware, costly.
3	RFID	Wenjie Ruan et al. [15] presented the idea of detecting human activity by using passive RFID. The system works on both RSSI signal and HOI events to locate the human.	Wireless, large area coverage.	Costly devices, The performance of RSSI decreases dramatically in many complex situations due to the presence of fading, scattering etc.
4	UWB	Ni. et al. [16] used ultra-wideband (UWB) tags with a Flexiforce sensor (FFS). In this you detect the location by ultra-wide-band sensors. On the patient they used 6 UWB wearable tags where location was determined by ultra-wideband sensors. Six UWB wearable tags were used on the patient's	Cost effective	Patient has to wear tags, Problem of two system integration, too much devices.

All of the approaches are used for measuring the hypertension, pre-eclampsia or eclampsia, but the problem is that no one explained the physical condition related to eclampsia such experiencing seizure episodes. G. Williams et al. [11] presented sensor sleeve but the patient has to wear the sleeve for monitoring purpose. During the pregnancy, if the patient has hypertension and not treated on time, then eclampsia might be experienced with severe effects and consequently it becomes difficult for a woman to wear any device during this critical condition. The existing methods did not clearly explain the detection of eclampsia and its onsets. As onset must be measured after its clear that patient is eclamptic otherwise this leads to the death of a patient.

The aim of this study is to monitor the body movements of an eclamptic woman using 5G sensing that leverage the perturbation of wireless channel using low-cost small wireless devices.

4. Multipath Challenges

The network interface card used in this work is dual a band PCI, that monitors the signal variations by capturing the WCI of all the sub-carriers. The reflection of the signal from the surroundings produces the multiple copies of the signal which then received by the transmitter through M distinct paths. The radio signals follow the M different paths to reach to the receiver and represent the channel frequency response *H (A, t)* as,

$$H(A,t) = e^{-j2\pi\Delta At}\sum_{k=1}^{M} bk(A,t)e^{-j2\pi A\tau_k(t)} \tag{1}$$

Where *bk(A,t)* represents the complex values for the initial phase offset and attenuation of the k^{th} path, $e^{-j2\pi A\tau_k(t)}$ represents the k^{th} paths phase shift with the $\tau_k(t)$ as the propagation delay. The $e^{-j2\pi\Delta At}$ represent the phase shift which then initiated due to the difference in carrier frequency ΔA from sender to receiver. The phase of the wireless signal is directly proportional to the change in the path length. By observing the Figure 4, where the signals are being reflected by the obstructions on the k[th] path. As the human body moves and covers the small distance with in time interval of 0 to t, it induces the change in k[th] path length from l_k *(0)* to l_k *(t)*. The wireless signal propagates with the speed of light c, so we can write the $\tau_k(t)$ as $\tau_k(t) = l_k(t)/c$. The λ and f represents the signal wavelength and the carrier frequency and hence $\lambda = c/f$ so the previous phase shift $e^{-j2\pi A\tau_k(t)}$ can be rewritten as $e^{-j2\pi l_k(t)/\lambda}$. This transformation shows that single wavelength changes the path length and the received subcarrier experiences 2 π phase shift.

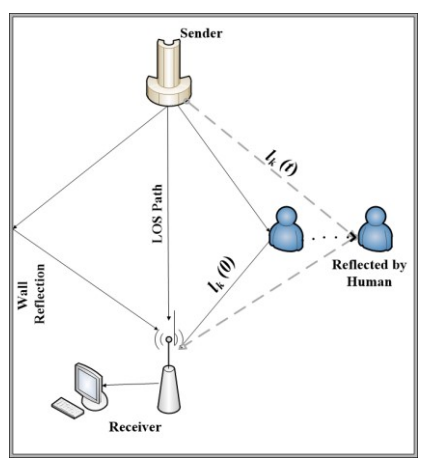

Figure 4: Signal visual representation

5. Data classification schemes implementation

In this work, the classification of data holds an important position and for that we have used four data classification methods known as Support Vector Machine (SVM), K-Mean, K-Nearest Neighbor (KNN) and Random Forest (RF). We also compared the four algorithms and concluded that SVM shows better performance than the other three algorithms.

Machine learning (ML) is the field of study that gives computer the ability to learn without being explicitly programmed [20]. It is about building a compressed representation of data. ML is of two types supervised and

unsupervised and SVM falls in the category of supervised ML. In this way, we can make predictions from our data by using SVM algorithm. There are other energy efficient algorithms for received wireless data [17] but we choose SVM. The SVM primarily works on two classes and is a discriminative classifier formally defined by separating hyperplane. The hyperplane serves as a decision boundary for classification of datasets between two classes. This data consists of data instances and represented as feature vectors. There exists some closest points to the hyperplane called the support vectors and are expressed as:

$$w^T u + b = 0 \tag{2}$$

Here w represents the weight vector, u is the input vector and bias is represented by b. The distance between u and the hyperplane is given as:

$$\frac{\left|b + w^T u\right|}{\|w\|} = \frac{1}{\|w\|} \tag{3}$$

Where the margin is the twice the distant to the closest vector,

$$\frac{2}{\|w\|} \tag{4}$$

For making the decision boundary, we specify the decision rule for that, a vector is considered of any length to the line perpendicular to the median as shown in Figure 5,

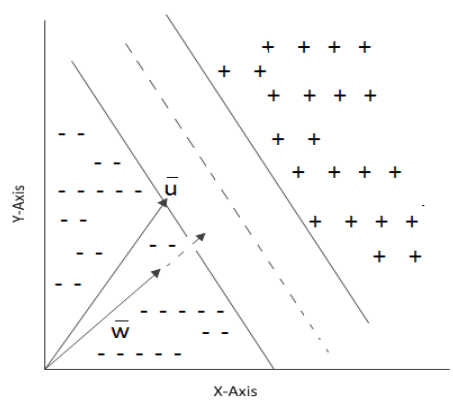

Figure 5: SVM classification.

$$\bar{w}.u + \bar{b} \geq 0 \tag{5}$$

Equation (5) represents the decision rule now for positive and negative samples the equations will be,

$$\begin{aligned} \bar{w}.\bar{x}_+ + b &\geq 1 \\ \bar{w}.\bar{x}_- + b &\leq 1 \end{aligned} \tag{6}$$

Now we introduce another variable y_i which will correlate to two classes as, $y_i = +1$ for positive samples and $y_i = -1$ for negative samples. Such that equation (6) will becomes,

$$y_i(\bar{w}.x_i + \bar{b}) \geq 1 \tag{7}$$

for i = 1, 2... k

Now maximizing the width of the two decision boundaries we will use the Lagrange transform in which we will use the lagrangian multiplier

$$L = \frac{1}{2}\left\|\bar{w}\right\|^2 - \sum \alpha_i [y_i(\bar{w}.\bar{x} + b) - 1] \tag{8}$$

After differentiating w.r.t $\bar{w}$ we get the value for $\bar{w}$ as,

$$\bar{w} = \sum_{i=1}^{m} \alpha_i y_i \bar{x}_i \tag{9}$$

$\bar{w}$ Is the linear sum of the vectors shown in equation (9). After further solving the equation (8) for further differentiating w.r.t to b and after substitution we get,

$$L = \sum \alpha_i - \frac{1}{2}\sum\sum \alpha_i \alpha_j y_i y_j (x_i.x_j) \tag{10}$$

In this way the optimization depends on the dot product of the pairs of samples like $(x_i.x_j)$ and finally the decision rule for the decision boundary is,

$$f(x) = \sum \alpha_i y_i (\bar{x}_i.\bar{u}_i) + b \geq 0 \tag{11}$$

The variable x is the input vector, u is any unknown vector and, α_i is used for the support vectors to be defined among all the inputs.

On the other hand, if the feature vectors are not separable in lower dimensions, then we have to cast them to higher dimensions by using kernel functions. The mapping function $\varphi(\bar{x})$ is used for the classification process by utilizing the linear hyperplane.

$$\varphi(\bar{x}_i).\varphi(\bar{x}_j) \tag{12}$$

The kernel functions provide the dot product of the vectors to the higher space and will reduce the intricacy of numerical optimization in that higher space.

$$K(x_i, x_j) = \varphi(\bar{x}_i).\varphi(\bar{x}_j) \tag{13}$$

In general, SVM uses many kernel functions for the classification of nonlinear patterns, which are polynomial sigmoid, linear, radial basis functions (RBF) etc are also known as the parameters for the algorithm. In this work we used three kernel functions (linear, polynomial and RBF). The mathematical expressions of these kernel functions are shown in Table 3.

Table 3: Inner-Product Kernel functions.

Type	**Kernel Function** $S(x, x_i)$, i =1,2,3,…P
Linear	$X^T X_i + C$
Quadratic	$(X^T X_i + C)^d$
Radial-basis function (RBF)	$e^{\left(-\frac{\|X - X_I\|^2}{2\sigma^2}\right)}$

The total 200 samples we used for the training of the classifier and 100 for the testing purpose. We will explain in the following sections.

The Steps involved in the whole classification process are explained as follow,

Algorithm: Steps for Classification of extracted wireless data.

Step 1: Classification function *f(x)* evaluation. Defined as, $f(x) = sign(w^T x + b)$. Where w^T along with b represents the classification surface function parameters, x is the feature extracted from the available amplitude data.

Step 2: Introduces the y with the value of 1 and -1 for representing two categories slightly different from each other. In this 1 means for Wi-Wheat and -1 means abnormal. Added the w a normal vector as a constraint and α the Lagrangian multiplier expressed the new formulation represented as follow, $L(w,b,\alpha) = \frac{1}{2}\|w\|^2 - \sum_{i=1}^{n} \alpha_i (y_i (w^T x_i + b) - 1)$, where $L(w,b,\alpha)$ known as the objective function, n represents the overall size of the training set.

Step 3: To find the values for w and b we followed the maximum dividing line in this way we optimized the two parameters. The classification can be done by following equation,

$$\max |W(\alpha)| = \sum_{i=1}^{n} \alpha_i - \frac{1}{2} \sum_{i,j=1}^{n} y^{(i)} y^{(j)} \alpha_i \alpha_j \langle x^{(i)}, x^{(j)} \rangle$$

$s.t.: 0 \le \alpha_i \le C$, $i = 1, 2 \ldots n$

And also $\sum_{i=1}^{n} \alpha_i y^{(i)} = 0$. In this C represents the penalty coefficient.

Step 4: In every iteration α_i and α_j are selected and the others remain at constant. In this way we obtained the hyperplane with maximum margin as,

$f(x) = sign\left(\sum_{i=1}^{n} y_i \alpha_i K\langle x^{(i)}, x \rangle + b \right)$, in this the K represents the polynomial kernel function for mapping the data in the higher dimensions and is represented as,

$K\langle x^{(i)}, x \rangle = (\langle x^{(i)}, x \rangle + c)^d$, In this d is representing the degree of polynomial kernel function.

The RBF kernel function can be represented as,

$K\langle x^{(i)}, x\rangle = \exp\left\{-\frac{1}{2\sigma^2}\left\|x - x^{(i)}\right\|^2\right\}$, Where σ represents the standard deviation.

We have calculated the confusion matrix for the four classifiers. The confusion matrix gives the performance overview of an algorithm. It shows the true values of data and identifies the errors. Also, it summarizes all of the predictions made by the classifiers for the particular classes. The confusion matrix for SVM classifier is shown in Table 4. There are total four classes as shown in the Table 4, each body motion represents a separate class.

Table 4: SVM Confusion Matrix.

Class (A1, A2, A3, A4)	**SVM Confusion Matrix with 200 samples**			
	Sitting	Lying	Walking	Seizures
Sitting	**193**	1	0	5
Lying	3	**199**	0	5
Walking	2	0	**200**	2
Seizures	2	0	0	**188**

The other classifier known as Random forest was also used in the classification process. RF classification algorithm works on predictors and reduces the computational cost and enhances the classification performance. On the available data RF makes the regression trees with the help of randomized features. These trees specify the split on every node. The parameters such as n_estimator was set to the higher values, which specifies maximum number of tress and n-job was set to -1 means no restriction of using number of processors. The overall CPU communication reduces by using this algorithm and it provides the parallel computation to enhance the computational performance. The Table 5 shows the confusion matrix for RF algorithm for comparison with other algorithms.

Table 5: RF Confusion Matrix

Class (A1,A2,A3,A4)	**RF Confusion Matrix with 200 samples**			
	Sitting	Lying	Walking	Seizures
Sitting	**190**	8	1	10
Lying	7	**182**	5	5
walking	0	5	**193**	6
Seizures	3	5	1	**179**

KNN classifier gives us the suitable results. As it is clear from the name nearest neighbour, from all of the available feature space KNN specifies the nearest sample. All of the nearest neighbours give the majority votes for the classification of the available data. KNN specifies the common class and assigned the data set to it for the classification. KNN algorithm set the parameter which is known as distance functions e.g, if $K = 1$ then the available dataset lies in the nearest neighbour class. KNN utilizes three distance functions in this work. On the other hand Hamming distance works only on the availability of categorical variables. In KNN noise is directly proportional to the value of K. Increasing the value of K reduces the effect of noise on the given dataset. Table 6 represents the confusion matrix for KNN algorithm to specify its performance for the classification of available dataset.

Table 6: KNN Confusion Matrix

Class (A1,A2,A3,A4)	**KNN Confusion Matrix with 200 samples**			
	Sitting	Lying	Walking	Seizures
Sitting	**180**	6	8	14
Lying	8	**175**	2	8
walking	4	8	**188**	7
Seizures	8	11	2	**171**

The three distance functions used and also the hamming distance are shown in the Table 7.

Table 7: KNN Distance Functions.

Distance Functions	**Formula**
Manhattan	$\sum_{i=3}^{k} \lvert x_i - y_i \rvert$
Minkowski	$(\sum_{i=1}^{k} \lvert x_i - y_i \rvert^{q})^{1/q}$
Euclidean	$\sqrt{\sum_{i=1}^{k} (x_i - y_i)^2}$
Hamming Distance	$D_H = \sum_{i=1}^{k} \lvert xi - yi \rvert$

We also utilized the clustering algorithm known as K-mean algorithm. It's an iterative algorithm. It always assumes the Euclidean space and the Euclidean distance. We adjusted the parameter K = 4 as the number of clusters will be four according to the four body motions. All these four clusters are then initialized by picking one point per cluster. Data points then assigned to each cluster by placing the chosen points to the closest centroids for each cluster. The confusion matrix explains the classification comparison with other classifiers. Table 8 shows the confusion matrix for K-mean algorithm.

Table 8: K-mean Confusion Matrix

Class (A1,A2,A3,A4)	**K-Mean Confusion Matrix with 200 samples**			
	Sitting	Lying	Walking	Seizures
Sitting	**196**	8	7	15
Lying	1	**172**	6	10
walking	2	10	**180**	10
Seizures	1	10	7	**165**

6. Classification scenario of SVM

The obvious choice from all the classifiers is the linear classifier known as SVM, which is also used for the classification of the available objects to the available classes. So each object has its specific class and the available data set for the classes, will train the classifier. As the classifier is trained now each class has the right data set for classification. Testing phase is also important where the classifier is used for testing data and its performance is evaluated by making comparison on the classification of that testing data. In this work there are four types of body motions of the patient which acts as a class and producing a trace from a single receiver. The single trace from four classes acts as an object which needs to be classified. The classifier used here works in a multidimensional space know as feature space. In feature space different points represents the objects and the coordinates for these points act as the object's features values. These features are the significant quantity for the given objects and are normalized to adjust the points in the feature space within the hypercube. Compatibility of features is the important issue in the classification process and for avoiding the computational complexity; we choose the smaller number of features. So SVM separates the two data classes on the basis of linearity to identify the hyperplane, which is the separation line between the two different classes of data in the feature space. Thus maximum margin hyperplane is achieved as by maximizing the distance on both sides of hyperplane from the marginal data points. Quadratic programming helps hyperplane to make some computations, which is an adequate optimizing technique. In this SVM soft margins are used to classify the datasets which are not apparently separable by hyperplane. In this way algorithm accommodate the large margin and some misclassified points. Secondly the nonlinear kernel functions are used to map the classes which are nonlinearly separable into the high dimension feature space [18]. The block diagram of the SVM implementation is shown in Figure 6.

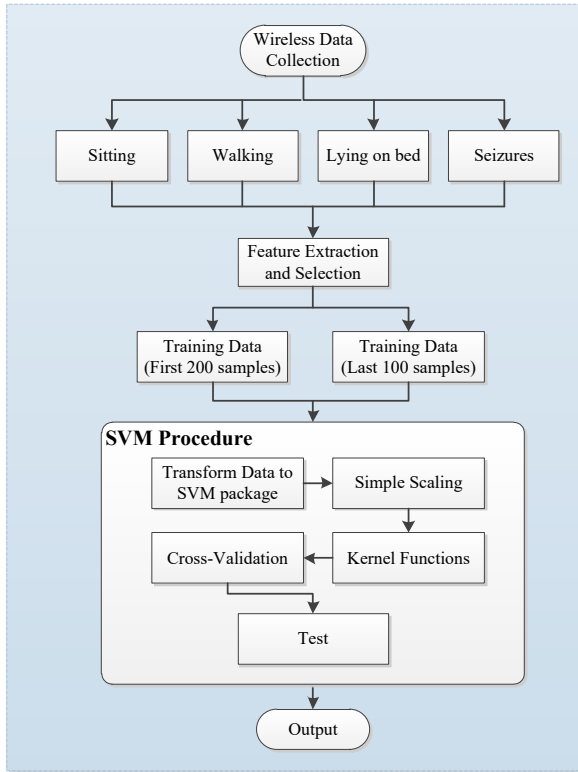

Figure 6: Block diagram for SVM-based classifier.

7. Results discussion

In this portion we explain the idea behind the experiment using the 5G wireless sensing [6-7]. The experimental setup used in this research is very low cost, which includes the simple wireless devices easily compatible with the modern communication standards. The wireless transmitter operating at frequency of 4.8GHz used as an access point (AP). A Lenovo desktop computer ingrained with ASUS ACE 100 4 x 4 (ASUS PCE-AC88) dual band PCI, act as a wireless device connected to the AP. The approximated distance between the transmitter and receiver was adjusted around 4 meters.

This procedure took place in the conference room of Xidian University to observe the body movement of a patient as shown in Figure 1. For the collection of data, pinging of the AP is done at 5 packets per seconds to collect the data at client side with modified driver. Multipath exits in this wireless scenario which changes the collected data due to change in the location. In the present scenario, the transmitter sends some packets of data and at the receiver side we get the data represented in the form of matrix H. This matrix is called channel frequency response (CFR) and has the size of 30 x 1. The rows in the CFR specify the sub-carrier frequencies and columns imply the receiving antenna. The general CFR could be shown as,

$$CFR = [CFR(1), CFR(2), ..., CFR(m)] \tag{13}$$

As discussed earlier, the CFR is a matrix of size 30 x m , where m represents the received packets. The rows in the CFR matrix show the observed changes in the signal information over the given sub-carriers. The Figure 6 represents the CFR data in raw form as per packets received. This raw data represents the four body movements of a

person. The Figure 7 also contains the phase information for all of the four body movements. The green part is the random phase information and the red part explains and shows the sanitized phase information of each body motion. As we can clearly observe the seizures shows more scattering in the sanitized part of the phase information.

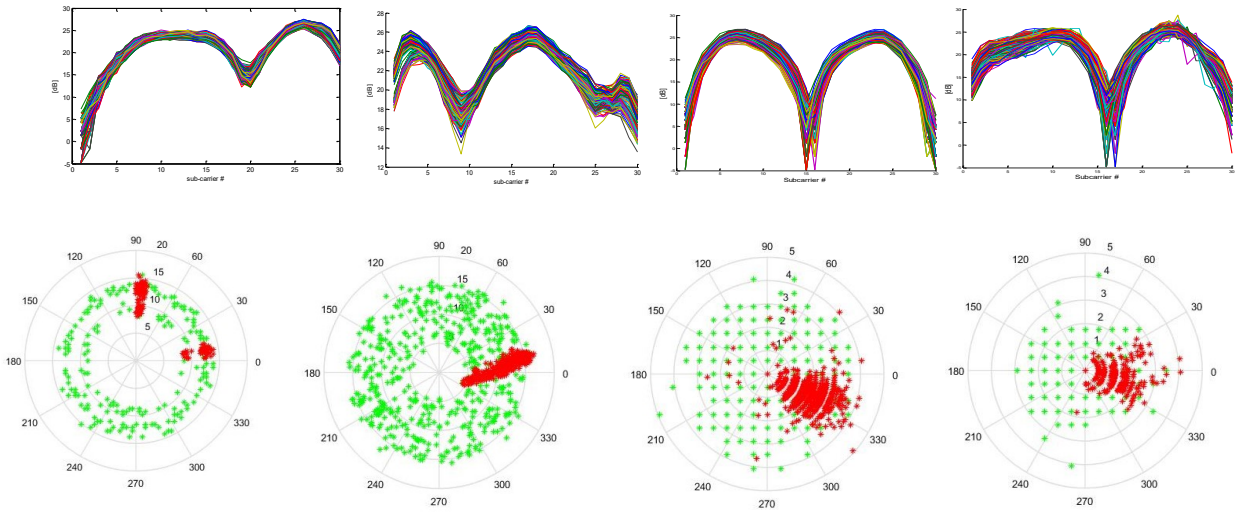

(a)Sitting (b) lying (c) Walking (d) Seizures

Figure 7: Measured amplitude history for CFR in experiment

The Figure 7 shows the frivolity in CFR amplitude for four body motions of the subject. The four body motions clearly showing the changes in CFR for sitting on a chair, walking, lying on a bed and seizures. Changes could easily be shown in the CFR but to clearly observe them, we choose the sub-carrier number fifteen as from this sub-carrier on ward time and amplitude variation become easy to observe. The choice of the particular sub-carrier is due to scrutinize the maximum change and difference between the comparable sub-carriers, as Figure 8, shows the different body motion and their changes in amplitude and time.

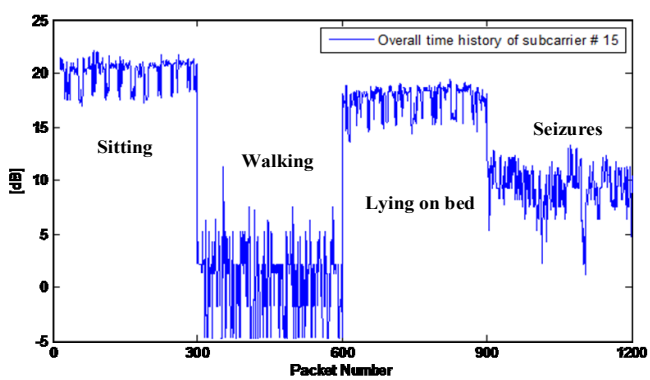

Figure 8: The CFR of four body motions.

Figure 8 indicates the CFR registration of four body motions for total 1200 packets of data. The 300 packets of data for each body motion and approximately subject stayed in these positions for 2 minute each. The extensive shift in CFR came in the position of seizures. We also kept in mind and treated the obstacles between the transmitter and receiver as a system part. Through these obstacles, reflection, refraction, and scattering appears and also

considered as major part in the experiment. We also kept in mind the power for transmitting the data as [24] also shows the promising results related to that issue. From the Figure 7, we can see that the power levels for walking and seizures are overlapping somehow which must be differentiated in order to detect the correct body movement. This system shows the feasibility of using non wearable devices, although some wearable devices showed promising results like [25]. In our research we focused on non wearable solution for human activity detection and we used SVM with KNN, RF and K-Mean for the classification of these four classes to detect the correct body movement.

This work uses *svmtrain* (built-in function in Matlab) for the training of SVM. For each class this *svmtrain* works on *one-versus-rest* approach. The default value for cost parameter C (C=1) was adjusted. The optimal decision boundary was adjusted by applying the sequential minimal optimization (SMO) solver. For each class 2 sets of features were used to train the SVM, one considering 5 features per class and other with all the 10 features. The amplitude information is regarded as the data for training and testing. We get 300 samples for each of four classes, each samples consisting of 30 data elements. Out of 300 samples, the first 200 samples from each class were used for training, while the last 100 samples of each class were used for testing the SVM. For the training of each of the cases three Kernel functions were used namely as linear, polynomial, and the radial-basis (RBF) as mentioned before. At the beginning 5 features were used to observe the accuracy for all of the cases. At the last 10 features were used to delve into the accuracy of the SVM.

Table 9: Accuracy rate of SVM with 200 samples of each class.

Kernel	**5 Features**	**10 Features**
Function	**C1 C2 C3 C4**	**C1 C2 C3 C4**
Linear	92.75 97.50 100 88.50	93.75 99.00 100 92.25
Polynomial	96.75 98.50 100 94.25	97.75 98.75 100 97.75
RBF	96.00 99.00 100 93.75	96.75 99.25 100 94.00

The Table 9 shows the total accuracy rate of different kernel functions in SVM with 200 samples for training of each class. There are total four classes so three kernel functions, linear, Polynomial and RBF were used to calculate the accuracy rate for each class. As shown in the Table 9, firstly accuracy was measured with 5 features and then with 10 features for all of the four classes using three mentioned kernel functions. Cross validation is very important for the reliability performance of any algorithm. We used 5-fold cross validation to train the SVM. In this the data then divided into 5 subsets. Each was held out in turn as the validation set, while the other four datasets do training set and train model, and then we calculated *Erri* of the model in the test set. After that, the average of 5 *Erri* was calculated to get the last *Erri.* As shown,

$$CV_{(k)} = \frac{1}{k}\sum_{i=1}^{k} Err_i \tag{14}$$

Err_i represents the number of misclassifications of the i^{th} model on the i^{th} test set.

This total accuracy has the definition of ratio of correct classifications to the all test samples for the given classes. The accuracy increases with the increase of the features as shown in Table 9. In this work, the ten time-domain

statistical features are used, as shown in Table 10. The Table 10 shows all of the 10 features used for training and testing of the SVM.

Table 10: Ten Features used for SVM

$(Y_{MV}) = \frac{1}{N}\sum_{i=1}^{N} x_i$	$(Y_{STD}) = \sqrt{\frac{1}{N}\sum_{i=1}^{N}(x_i - \mu_x)^2}$
$(Y_{RMS}) = \sqrt{\frac{1}{P}\sum_{i=1}^{P} x_i^2}$	$(Y_{SRA}) = \left(\frac{1}{N}\sum_{i=1}^{N}\sqrt{\lvert x_i \rvert}\right)^2$
$(Y_{KV}) = \frac{1}{P}\sum_{i=1}^{P}\left(\frac{[x_i - \mu_x]}{\sigma}\right)^4$	$(Y_{SV}) = \frac{1}{P}\sum_{i=1}^{P}\left(\frac{[x_i - \mu_x]}{\sigma}\right)^3$
$(Y_{CF}) = \frac{\max(\lvert x_i \rvert)}{Y_{rms}}$	$(T_{PPV}) = \max(x) - \min(x)$
$(Y_{IF}) = \frac{\max(\lvert x \rvert)}{\frac{1}{P}\sum_{i=1}^{P}\lvert x_i \rvert}$	$(Y_{MF}) = \frac{\max(\lvert x \rvert)}{Y_{SRA}}$

The accuracy achieved by the kernel functions is shown in Table 9 and the progress with the polynomial and RBF is comparatively better than linear kernel function. By using linear kernel function the progress was there for few features but not increases progressively as compared to Polynomial (quadratic) and RBF. The SVM used in this work shows the characteristics of using 10 features, 200 training samples with 100 testing samples for each class. For the normal class, training of data samples was done as positive values and for other classes as negative or false values. From the Table 8 we can conclude that accuracy increases by increasing the number of features used for training SVM. We can see this graphically in Figure 9, as also mentioned in Table 9,

(a) Accuracy of SVM using linear kernel function.

(b) Accuracy of SVM using Polynomial kernel function.

(c) Accuracy of SVM using RBF kernel function

Figure 9: Classification performance of SVM for different body motions.

8. Feature extraction &selection

Further, the raw data obtained from the proposed method was not sufficient for the four body motions. From Figure 7(b) and 7(d), there is a higher similarity between walking and seizures. Therefore, the data was preprocessed to extract features that were able to identify and classify the four body motions. The reliable monitoring performance is highly dependable on the selection of the features so we must select the reliable features which shows better separability as the number of classes increases [21]. Features can be extracted from time-domain analysis, frequency-domain analysis, or time-frequency-domain analysis. Time domain features can easily be extracted and have sufficient information for a motion. As time domain features are already mentioned in Table 9.

In our work for reliable selection of features and for their screening, we used fisher's discrimination ratio [19]. Fisher's linear discriminant is a method to find a linear combination of features that separates two or more classes of objects. Larger the Fisher's ratio, greater the distance between two classes. Fisher's discriminant is formulated as follow:

$$J = \frac{(\mu_1 - \mu_2)^2}{s_1^{\,2} + s_2^{\,2}} \tag{15}$$

here μ_1 and μ_2 are the means of walking class and seizures class, s_1^2 and s_2^2 are respective variances.

Fisher's ratios are then calculated for all candidate features, the results of which are shown in Figure 8. Features 2, 4, 6, 9 and 10 have higher ratios, indicating that they can provide better separability between each class. As a result, these features are chosen for monitoring tool conditions. Space plots of feature 4, 9 and 10 are shown in Figure 10, which indicates good class separability.

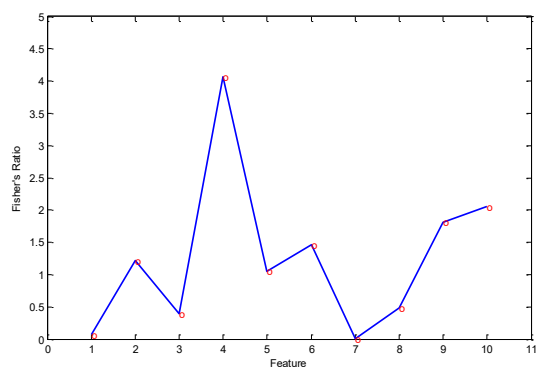

Figure 10: Fisher's ratio plot for all candidate features.

To observe the performance of SVM we need to consider the desirable number of features to extract the exact information from the given set of data from different classes. As explained the linear kernel functions shows less accuracy in most of the cases as compared with Polynomial and RBF. The accuracy improves in Polynomial and RBF with percentage of more than 4% with 5 features and 1% to 2% for 10 features.

In SVM many features are shown but only the best features with better performances were chosen to show different actions in feature space as mentioned earlier. We considered time-independent statistics involving mean value μ, standard deviation σ and kurtosis.

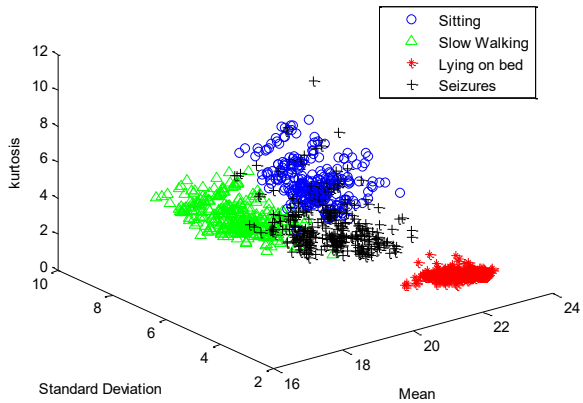

Figure 11: Different actions in feature space.

SVM classified the group of data into their particular class. Figure 11 shows the exact distribution of data into four classes which are representing the four body motions. All the motions were classified deeply to see the difference between each body motion [19]. We also checked and classify these groups of data using other Algorithms known as K-mean clustering, KNN and RF.

9. Performance analysis of algorithms

This section describes the classification of the data collected from the C-Band WCI. We classify the data by using four algorithms, SVM, KNN, RF and K-mean. The result from these algorithms was then examined by using six performance matrices, which are precision, recall, F-measure, accuracy, specificity and Cohen's Kappa coefficient [22,23].The Table 11 shows the six performance metrics along with their formulas.

Table 11: Six Performance metrics

Performance Metrics	Formulas
Precision	$\frac{Tp}{Tp+Fp}$
Accuracy	$\frac{Tp+Tn}{Tp+Tn+Fp+Fn}$
Recall	$\frac{Tp}{Tp+Fn}$
Specificity	$\frac{T_n}{F_p+T_n}$
Kappa	$\frac{(Accuracy-Accuracy_{expected})}{1-Accuracy_{expected}}$
F-Measure	$\frac{2Tp}{(2Tp+Fp+Fn)}$

We have calculated the values for all of the six performance metrics by using 11 time domain features with RBF

kernel function and presented in the form of table in Table 12 and 13. We have used 200 samples for the training of classifier and 100 samples for the testing. Then we compared the results from all of the classifiers but our optimum choice was SVM due to its better accuracy. The accuracy increases with the increase of the feature vectors and the error rate is less in SVM as compared with other three algorithms.

Table 12: Classification results for SVM & RF.

Classes	**SVM Classification results (%)**					
	Accuracy	**Recall**	**Precision**	**Specificity**	**F-Measure**	**Kappa**
Sitting	96.5	97	96.9	98.1	97.4	
Lying	99	96.5	96.2	99.8	99	
Falling	100	98.5	98.6	99	98	0.97
Seizures	94	98.9	98.9	98.3	99.5	
Classes	**RF Classification results (%)**					
Sitting	95	90.2	90	93.2	93	
Lying	91	91	91.5	94.5	94.6	
Falling	96.5	94.5	94.6	95	96	0.90
seizures	89.5	95.2	95.2	96	96.2	

Table 13: Classification results for KNN & K-Mean.

Classes	**KNN Classification results (%)**					
	Accuracy	**Recall**	**Precision**	**Specificity**	**F-Measure**	**Kappa**
Sitting	90	86.5	86.5	90.2	92	
Lying	87.5	90	90.6	90	90	
Falling	94	91	90.8	88.8	89	0.85
Seizures	85.5	89.1	89.1	89.3	90.8	
Classes	**K-Mean Classification results (%)**					
Sitting	98	86.7	86.7	95.2	94	
Lying	86	91	91	92.5	91	
Falling	90	89	89.1	87	88	0.85
seizures	82.5	90	90.1	88.6	89	

From Table 12 and 13 we clearly see the difference between four classifiers by computing six performance metrics. SVM showed better result with greater number of features by showing maximum accuracy. The other classifiers also showed reasonable accuracies. The RF and KNN showed the values for specificity and F-Measure more than 90% but K-Mean clustering classifier values for these two metrics is more convenient and much better. The accuracy for the SVM is much better than other explained algorithms, as we can see that the accuracy for SVM is in between 95 to 100%, which specifies less error rate for this data. The average Kappa coefficient value for SVM is 0.97, and very close to 1 which is much better than other three. So in general SVM worked well for our data classification. The error rate in SVM is very low as already clear from the measurement of the accuracy. The accuracy in SVM increases with the usage of kernel parameter known as polynomial and RBF.

10. CONCLUSION

In this paper we monitored different body motions of the eclamptic patient to avoid the seriousness of the disease. Wireless sensing for monitoring the patient is very essential to overcome the drawbacks related to eclampsia. This research shows that by using very low cost equipment we can easily classify the body motion of the eclamptic patient. A simple SVM classifier is used to classify the data obtained from the sensors and data is divided into four classes depending upon the type of body motion. This research also shows the feasibility of using some other classifiers known as KNN, RF and K-mean. The cost on the classification is very low as features used are less expensive and expresses better identification. Efficiency of the classifier increases by using higher training data but to some extent. Furthermore SVM proved to be the better choice among all other classifiers being used in the research. This research focuses on the identification of various activities to detect the seizures in human body. In the future work we will move a step head in prediction of such diseases. We have tested our system for the identification of body movement to detect the seizures and it works well but in future we would try to build a system that can timely predict the seizures to prevent any serious injury to the patient.

ACKNOWLEDGEMENT

The work was support in part by Fundamental Research Funds for the Central Universities (JB180205), in part by the International Scientific and Technological Cooperation and Exchange Projects in Shaanxi Province (Grant No 2017KW-005), in part by the China Postdoctoral Science Foundation funded project (Grant No. 2018T111023), in part by the National Natural Science Foundation of China (Grant No. 61671349 and 61301175).

REFERENCES

[1] Yulong Cai, Zhijin Qin, Fangyu Cui, Geoffery Ye Li and Julie A. McCann. “Modulation and Multiple Access for 5G Networks,” *IEEE Communications Surveys & Tutorials (Volume: 20 , Issue: 1 , Firstquarter 2018), PP 629 – 646, DOI: 10.1109/COMST.2017.2766698.*

[2] “Touching lives through mobile health: Assessment of the global market opportunity,” White Paper, GSMA, February 2012.

[3] “Q. N. Lu, J. J. Yang, D. Z. Chen, M. Huang, " ”State of the art and challenges of radio spectrum monitoring in china,” *2016 URSI Asia Pacific radio science conference, Vol 52, issue 10, pp 1261 – 1267, Oct 2017, doi.org/10.1002/2017RS006409*

[4] Tan Wang, Gen Li, Jiaxin Ding, Qingyu Miao, Jingchun Li and Ying Wang.” 5G spectrum: Is China Ready?” *IEEE communiation Magazine, July 2015 Volume: 53 , Issue: 7, pp 58 – 65, DOI: 10.1109/MCOM.2015.7158266*

[5] Leona c. Poon and Kypros H. Nicolaides. “Early Prediction of Preeclampsia,” Obstetrics and Gynecology International, Volume 2014, Article ID 297397*, pp 1 -11,doi: 10.1155/2014/297397*

[6] L. Duley, “ The global impact of pre-eclampsia and eclampsia,” Seminar in Perinatology, Vol 33, no. 3, (pp. 130-137, 2009).

[7] John Fance, Projestine S. Muganyizi. “ Characteristics of symptoms of imminent eclampsia: Acase referent study from a tertiary hospital in Tanzania,”Open Journal of Obstetrics and Gynecology, 2012, 2, (311-317).

[8] Akshay Jawaharlal Bhandari, Surekha V. Bangal, Pratik Y. Gori. “Ocular fundus changes in pre-eclampsia and eclampsia in a rural set-up,” Journal of Clinical Opthalmology and Research- Sep-Dec 2015, Vol 3, Issue 3. DOI: 10.4103/2320-3897.163264.

[9] Dustin T. Dunsmuir, Beth A. Payne and Garth Cloete. “Development of mHealth applications for Pre-eclampsia Triage,” IEEE Journal of Biomedical and Health Informatics, Vol. 18, no. 6, November 2014.

[10] Mario W. L. Moreira, Joel J. P. C. Rodrigues, Antonio M. B. Oliveira. KashifSaleem and Augusto V. Neto. “An Inference Mechanism Using Bayes-based Classifiers in Pregnancy Care,” IEEE 2016, 18th International Conference on e-Health Networking, Applications and Services (Healthcom).

[11] G. William, G. R Jones and K. Doughty. "A Telemedicine system to detect pre-eclampsia," IEEE/EMBS, 19th International conference, Oct. 30th – Nov. 2, 1997 Chicago, IL.USA.

[12] Kumari L. Fernando, V. John Mathews, Michael W. Varner and Edward B. Clark. "Prediction of Pregnancy-Induced Hypertension using coherence Analysis, "IEEE International conference on Acoustic, Speech and Signal Processing, 2004. Proceedings (ICASSP '04). Vol. 5.

[13] Yantao Lu, and Senem Velipasalar, "Human activity classification from wearable device with cameras", IEEE *51st Asilomar Conference on Signals, Systems, and Computers, October 2017, Pacific Grove, CA, USA. DOI: 10.1109/ACSSC.2017.8335163.*

[14] Ting Fen Tan, Soo Sian Teoh, Jun Ee Fow and Kin Sam Yen, "Embedded human detection system based on thermal and infrared sensors for anti-poaching application", *IEEE Conference on Systems, Process and Control (ICSPC), December 2016, Bandar Hilir, Malaysia, DOI: 10.1109/SPC.2016.7920700.*

[15] Wenjie Ruan, "Unobtrusive human localization and activity recognition for supporting independent living of the elderly", *IEEE International Conference on Pervasive Computing and Communication Workshops (PerCom Workshops), March 2016, Sydney, NSW, Australia, DOI: 10.1109/PERCOMW.2016.7457085.*

[16] H. Ni , B. Abdulrazak , D. Zhang , S. Wu , X. Zhou , K. Miao and D. Han "Multi-modal non-intrusive sleep pattern recognition in elder assistive environment" *Proc. 10th Int. Conf. Smart Homes Health Telematics, pp. 132-139, 2012.*

[17] Ali Hassan Sodhro, Li Chen, Aicha Sekhari, Yacine Ouzrout, and Wanqing Wu, "Energy efficiency comparison between data rate control and transmission power control algorithms for wireless body sensor networks", *International Journal of Distributed Sensor Networks (IJDSN), Vol.14, No.1, pp.1-18, 2018.*

[18] X. Yang, Syed Aziz shah, Aifeng Ren, Dou Fan, Nan Zhao, Shufeng Zheng, Weigang Wang, Ping Jack Soh, and Qammer H Abbasi, "S-Band Sensing-Based Motion Assessment Framework for Cerebellar Dysfunction Patients," in IEEE Sensors Journal. doi: 10.1109/JSEN.2018.2861906.

[19] S. A. Shah, Nan Zhao, Aifeng Ren, Zhiya Zhang, Xiaodong Yang, jie Yang, and Wei Zhao., "Posture Recognition to Prevent Bedsores for Multiple Patients Using Leaking Coaxial Cable," in IEEE Access, vol. 4, pp. 8065-8072, 2016. doi: 10.1109/ACCESS.2016.2628048

[20] X. Yang, Syed Aziz Shah, Aifeng Ren, Nan Zhao, Dou Fan, Fangming Hu, Masoor ur Rehman, Karen M. VonDeneen and Jie Tian, "Wandering Pattern Sensing at S-Band," in IEEE Journal of Biomedical and Health Informatics. doi: 10.1109/JBHI.2017.278759

[21] Tian Jing, Carlos Morillo, and Michael H. Azarian., "Motor bearing fault detection using spectral kurtosis-based feature extraction coupled with K-nearest neighbor distance analysis." *IEEE Transactions on Industrial Electronics* 63.3 (2016): 1793-1803.

[22] https://en.wikipedia.org/wiki/Precision_and_recall.

[23] https://en.wikipedia.org/wiki/Sensitivity_and_specificity.

[24] Ali Hassan Sodhro, Ye Li, Madad Ali Shah, "Energy-efficient Adaptive Transmission Power Control for Wireless Body Area Networks", *IET Communications, Vol.10, No.1, pp.81-90, Jan.2016.*

[25] Ali Hassan Sodhro, Arun Kumar Sangaiah, Gul Hassan Sodhro, Sonia Lohano, and Sandeep Pirbhulal, " An Energy-Efficient Algorithm for Wearable Electrocardiogram Signal Processing in Ubiquitous Healthcare Applications", *MDPI Sensors Vol.8, No.3, pp.923, 2018.*

Short Bios for all the authors:

1. Daniyal Haider is currently a PhD student with Xidian University.

2. Aifeng Ren is currently working with Xidian University.

3. Dou Fan is currently a master student with Xidian University.

4. Nan Zhao is currently a PhD student with Xidian University.

5. Xiaodong Yang is currently working with Xidian University.

6. Syed Aziz Shah was a PhD student at Xidian University and currently working with the university of Glasgow.

7. Fangming Hu is currently working with Xidian University.

8. Qammer H. Abbasi is currently working with School of Engineering, University of Glasgow.